Impact of Yttrium-90 Microsphere Density, Flow Dynamics, and Administration Technique on Spatial Distribution: Analysis Using an In Vitro Model

Marcus Caine, MPhil, Michael S. McCafferty, BSc, Scott McGhee, MSc, Pedro Garcia, PhD, Wayne M. Mullett, PhD, Xunli Zhang, PhD, Martyn Hill, PhD, Matthew R. Dreher, PhD, and Andrew L. Lewis, PhD

ABSTRACT

Purpose: To investigate material density, flow, and viscosity effects on microsphere distribution within an in vitro model designed to simulate hepatic arteries.

Materials and Methods: A vascular flow model was used to compare distribution of glass and resin surrogates in a clinically derived flow range (60–120 mL/min). Blood-mimicking fluid (BMF) composed of glycerol and water (20%–50% vol/vol) was used to simulate a range of blood viscosities. Microsphere distribution was quantified gravimetrically, and injectate solution was dyed to enable quantification by UV spectrophotometry. Microsphere injection rate (5–30 mL/min) and the influence of contrast agent dilution of injection solution (0%–60% vol/vol) were also investigated.

Results: No significant differences in behavior were observed between the glass and resin surrogate materials under any tested flow conditions (P = .182; n = 144 injections). Microspheres tend to align more consistently with the saline injection solution (r2 = 0.5712; n = 144) compared with total BMF flow distribution (r2 = 0.0104; n = 144). The most predictable injectate distribution (ie, greatest alignment with BMF flow, < 5% variation) was demonstrated with > 10-mL/min injection rates of pure saline solution, although < 20% variation with glass microsphere distribution was observed with injection solution containing as much as 30% contrast medium when injected at > 20 mL/min.

Conclusions: Glass and resin yttrium-90 surrogates demonstrated similar distribution in a range of clinically relevant flow conditions, suggesting that microsphere density does not have a significant influence on microsphere distribution. Injection parameters that enhanced the mixing of the spheres with the BMF resulted in the most predictable distribution.

ABBREVIATIONS

BMF = blood-mimicking fluid, RHA = right hepatic artery, VFM = vascular flow model

Locoregional therapy of liver tumors with yttrium-90 (^{90}Y) radioembolization has emerged as a significant treatment option for patients ineligible for curative therapy [1]. In ^{90}Y radioembolization, microspheres are injected into the hepatic arteries and mix with blood to be carried into the target tissue [2]. Although ^{90}Y radioembolization has been performed since the 1960s [3,4], there is still significant debate on its

technical considerations, including delivery technique and material ([5]). There are currently two commercially available microsphere products composed of resin (SIR-Spheres; Sirtex, North Sydney, Australia) and glass (TheraSphere; Biocompatibles UK, Farnham, United Kingdom), both of which comprise microspheres of similar size, but with different densities (resin, 1.6 g/cm^3; glass, 3.3 g/cm^3) ([5–7]). The difference in density has the potential to affect in vivo localization, although studies have shown no clinically relevant variation between anterior and posterior distribution of both material types ([5,8]). Uncertainty remains in regard to the mixing of the injected particles with the blood and their eventual distribution ([2,9,10]). The ability to predict microsphere distribution based on density and injection technique could enable enhanced dosimetry and ultimately treatment success ([11,12]).

The radiation dose from ^{90}Y microspheres is limited in range, with 50% of the absorbed dose within 2.5 mm of the microsphere ([2]). This necessitates final positioning of the microspheres close to their intended target and highlights the need for predicable distribution for maximum effect. Radioembolization is often administered in a proximal or lobar location, and it is an oversimplification to assume that the microspheres will mix homogeneously with the blood and then simply go wherever the blood goes, although this is often presented in flow-distribution studies ([13,14]). Factors thought to be significant for the prediction of distribution of microspheres include the size and density of the particles and the degree to which the particles will homogeneously mix with the blood during administration. When combined

with technologies such as dynamic computed tomography (CT) for imaging of vascular flow to allow an administration tailored to the patient's hemodynamic characteristics ([2]), there is potential to improve dosimetric control.

The objective of the present study was to investigate material density, flow, and viscosity effects and their influence on microsphere distribution within an in vitro vascular flow model (VFM) designed to simulate flow conditions within hepatic arteries. The central hypothesis is that radioembolic surrogate density will affect flow distribution.

MATERIALS AND METHODS

Experimental Setup

The VFM used for the present study was a silicone vascular cast (Elastrat Sarl, Geneva, Switzerland) with circular channel cross-sections, a 4-mm inlet, and six 0.9-mm outlets ([Fig 1]) ([15]). The inlet diameter was chosen to represent the hepatic vasculature at a typical injection point for ^{90}Y microsphere therapy at the right hepatic artery (RHA), and the outlet diameter is akin to that of a first-order hepatic bifurcation ([16,17]).

The VFM was oriented in the vertical plane (ie, perpendicular to the bench) to test density/gravitational influence on distribution and in the horizontal plane to evaluate the injection mixing. Inlet length was selected to ensure a fully developed flow profile from the catheter injection point before the first bifurcation (calculation presented in [Appendix A] [available online at www.jvir.org]) ([6,7,18–27]).
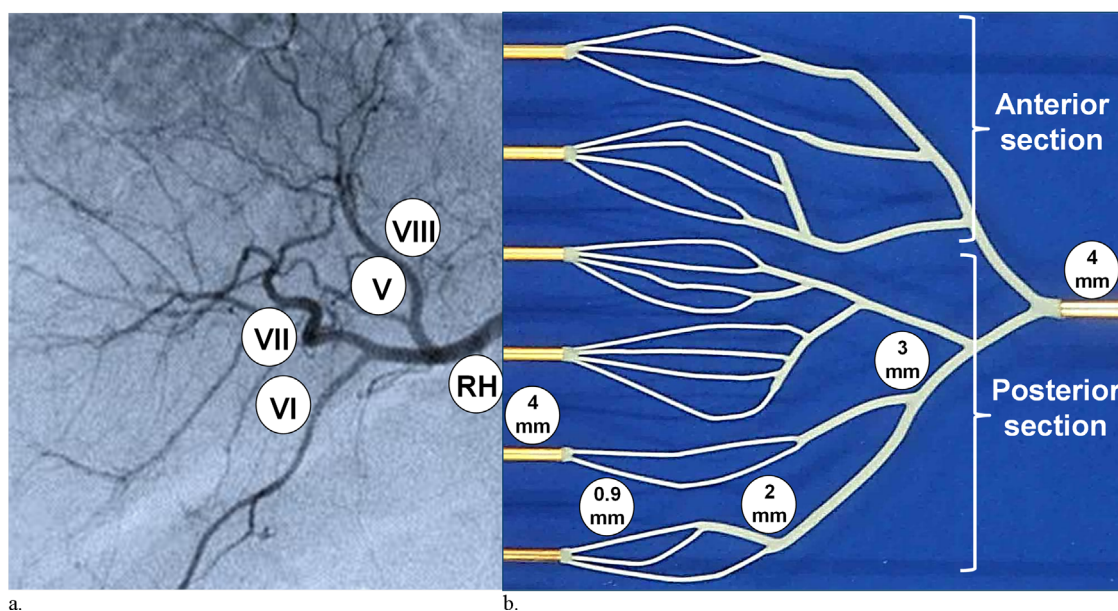

Figure 1. Comparison of **(a)** typical hepatic vasculature showing the RHA (*RH*) and the main arteries feeding liver segments V–VIII (angiogram adapted with permission from Kerlan [15]) and **(b)** VFM vessel orientation with anterior, posterior, and internal channel diameters labeled.

Microsphere Material Density and Injection Rate

Microsphere surrogates in saline solution were introduced via a 2.7-F, 110-cm Progreat microcatheter with a straight tip (Terumo, Tokyo, Japan) into the VFM inlet while blood-mimicking fluid (BMF) was circulating through the system (**Fig 2**). The catheter tip was radially centered and aligned with the axis of the channel, with its orientation visually confirmed before each injection to ensure repeatability. Catheter tip orientation was found to have a profound effect on microsphere distribution in previous simulations and in vitro studies (18–20). Injection rate was controlled with a PHD ULTRA syringe pump (Harvard Apparatus UK, Cambridge, United Kingdom).

To evaluate the influence of microsphere density, the injection rate was fixed at 20 mL/min in accordance with the package-insert instructions for use for glass microspheres (TheraSphere Yttrium-90 Glass Microspheres [package insert]. Farnham, UK: Biocompatibles UK Ltd: 2016.). This condition was selected instead of the less prescriptive resin injection methods consisting of "puff-like or pulsed injections" (SIR - Spheres microspheres [Yttrium-90 Microspheres] [package insert]. North Sydney, Australia: SirTex Medical: 2014.), as pulsed injection would have introduced additional variation to the results. To evaluate the effect of injection solution flow rate on mixing, constant injections were analyzed at 5-, 10-, 20-, and 30-mL/min rates (**Table**). These values cover the range of injection rates from the lowest recorded resin injection rate (5 mL/min) to the injection rate from the glass microsphere instructions for use (20 mL/min) (TheraSphere Yttrium-90 Glass Microspheres [package insert]).

Two nonradioactive microsphere surrogates were tested: resin microspheres (Aminex W50, Bio-Rad, Hercules, California; mean size, 32 μm; density, 1.6 g/mL) (6) and glass microspheres (mean size, 25 μm; density, 3.3 g/mL; BTG) (5,7). V-bottom vials were prepared with a standardized (settled) volume of microspheres per vial to remove volume-associated bias.

BMF Viscosity

BMF properties were selected to reproduce the kinematic viscosity of blood (28), in recognition that the viscosity of (non-Newtonian) blood will vary in vivo with blood pressure, ranging from 3.32 to 9.20 cP (18,29–31), and that viscosity is a key property affecting mixing and flow behavior. For the surrogate material density study, the BMF comprised a 44%:56% vol/vol glycerol:water mixture modified with 15% sodium iodide (28), yielding a dynamic viscosity of 4.51 cP (AMVn2-PA automated microviscometer, 1.8-mm capillary; Anton Paar, Ostfildern-Scharnhausen, Germany). For the investigation of the viscosity effect on mixing (**Table**), BMF with 20% vol/vol, 30% vol/vol, and 50% vol/vol glycerol dilutions were tested, yielding measured BMF viscosities of 3.03, 4.00, and 9.89 cP, respectively. This was intended to test the flow behavior over a range of in vivo conditions while using a Newtonian fluid.

BMF Flow Rate

The BMF was circulated through the inlet tubing and VFM with a DOSE IT P910 peristaltic pump unit (INTEGRA Biosciences, Zizers, Switzerland) at a nominal rate of 120 mL/min, chosen to approximate RHA flow at the lower end of reported ranges (120–559 mL/min) (18,31,32). **Appendix A** (available online at *www.jvir.org*) includes details of the measured pump pressure trace (**Fig E1** [available online at *www.jvir.org*]). BMF flow rate of 60 mL/min, intended to represent that in a sedated patient with low cardiac output, was also used to assess whether a lower BMF flow rate would accentuate the effects of particle density (21).

The injection solution was 0.9% saline solution (Fresenius Kabi, Oberursel, Germany) dyed with ~10 μg/mL vol/vol Safranin O dye (S2255-25G; Sigma Aldrich UK, Dorset, United Kingdom). The dye allowed visual assess-
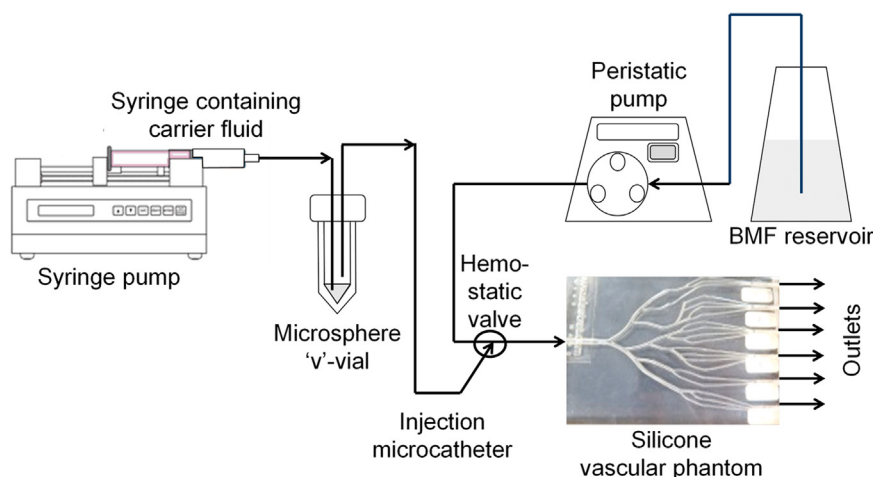

Figure 2. Schematic of experimental setup with device orientation not detailed.

ment of mixing and quantification of injection solution distribution (Cary Bio50 UV/Vis Spectrophotometer; Varian, Santa Clara, California) at the outlets. For the investigation of the viscosity effect on mixing, saline solution with 0%–60% vol/vol contrast agent (Omnipaque 350 Iohexol; GE Healthcare, Little Chalfont, United Kingdom) was used as the injection solution (Table).

Measured Outcome and Definitions

Replicates (n = 3) of each flow condition and surrogate type were performed. During each test, the effluent from each outlet was collected and the volume was measured as an indicator of flow direction. Each sample was diluted with BMF to an equal volume, and the dye concentration was measured by UV spectroscopy. The collected microspheres were then extracted, centrifuged,

and weighed for comparison by channel output with an analytical balance (MSA324s-1CE-DI; Sartorius, Göttingen, Germany). High-speed video was used qualitatively for flow-distribution monitoring (Fig 3). Microsphere "alignment" is defined as the microsphere weight percentage divided by the percentage BMF flow volume. Statistical comparison was made between surrogate materials by Student t test (two-sided, 95% confidence).

RESULTS

Effect of VFM Orientation

Glass and resin surrogates and injection dye were not significantly different between the vertical and horizontal orientations (20.05% vs 24.19% [$P = .0999$] and 17.21% vs

| Table. Test Plan for Investigation			
Objective	**Description**	**Test Setup**	**Outputs**
Microsphere density and gravitational effects	Vertical vs horizontal flow influence on microsphere distribution	Horizontal and vertical orientation, standard 120 mL/min flow rate and 20 mL/min injection rate, n = 3 replicates	Average dye, surrogate weight, and volume flow per channel
Relative injection flow rate	Effect of modifying BMF flow rate and injection rate on microsphere distributions	Horizontal orientation with varied injection rate and flow rate, n = 3 replicates	
Injection solution viscosity	Effect of altered BMF viscosity and modification of injection solution with 0%–60% vol/vol contrast agent	Horizontal orientation, standard 120 mL/min flow rate, standard 20 mL/min injection rate, modified BMF and injection viscosity, n = 3 replicates	

BMF = blood-mimicking fluid.
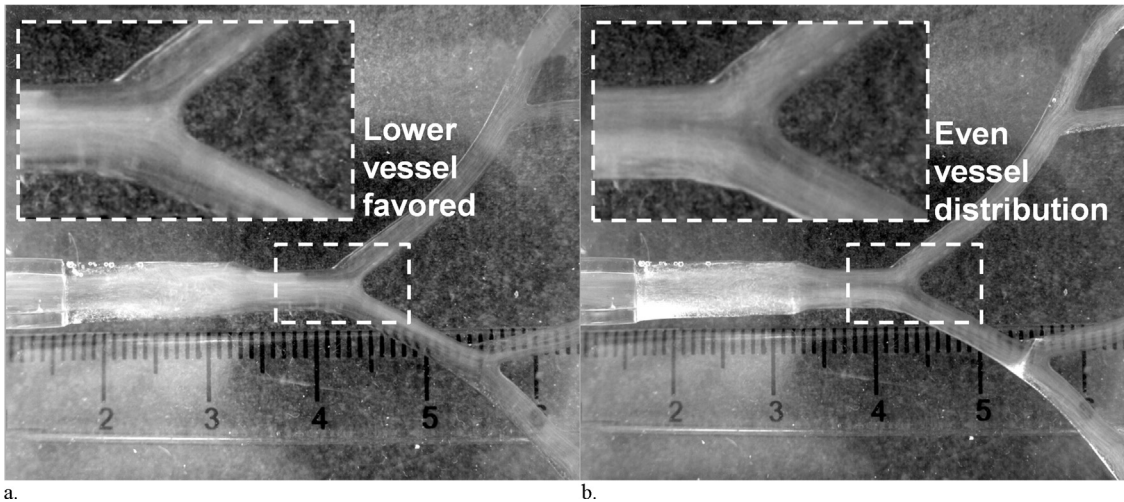
Figure 3. High-speed video still frames showing **(a)** developed flow profile for 5-mL/min injection with saline solution favoring lower vessels and **(b)** showing uniform mixing at primary bifurcation injected with saline solution at 20 mL/min. (Scale is in centimeters; inset shows 3× magnification of the primary bifurcation in the outlined area.)
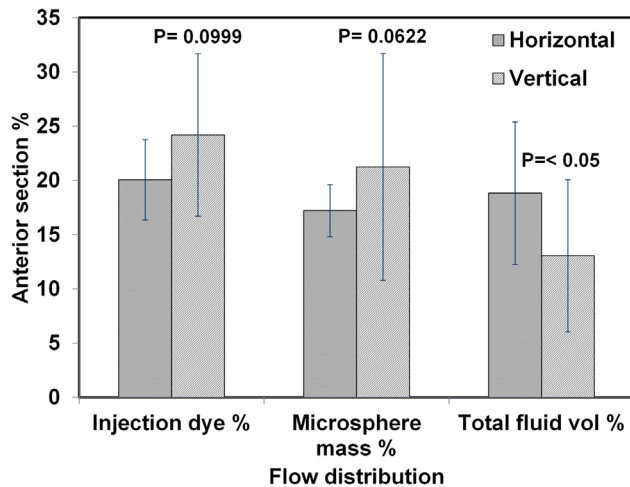
Figure 4. Anterior VFM channel dye, surrogate mass, and total fluid volume distribution by orientation (vertical and horizontal). Average percentage for 12 replicate injections of resin and glass surrogates with standard deviation is shown. Fluid volume presented the only statistically significant variation.
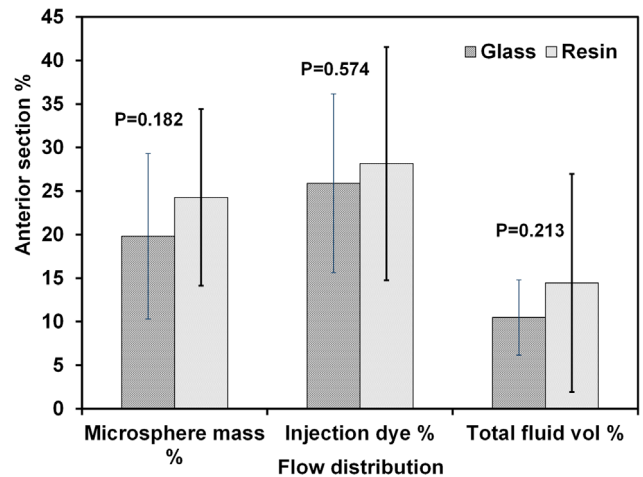

Figure 5. Anterior VFM channel distribution by surrogate material for weight, dye, and volume percentages, with an average of n = 18 with standard deviation shown. Testing performed in vertical VFM orientation shows no significant variation based on any parameter when comparing surrogate properties.

21.25% [$P = .0622$], n = 12; Fig 4). However, it was found that the total flow volume did distribute differently (18.83% vs 13.05%; $P < .05$; n = 12), with more total flow going to posterior vessels than anterior vessels.

Effect of Microsphere Density on Gravitational Sedimentation

A comparison of the resin and glass microsphere distributions in the vertical VFM orientation (to emphasize the influence of gravity; injection rate, 20 mL/min; BMF flow rate, 120 mL/min) demonstrated no significant difference between the materials as measured by dye concentration (25.89% vs 28.15%; $P = .574$; n = 12), microsphere weight (19.81% vs 24.26%; $P = .182$; n = 12), and total fluid volume (10.48% vs 14.44%; $P = 0.213$; n = 12; Fig 5).

Reducing the injection rate to 10 mL/min and BMF flow rate to 60 mL/min yielded no significant difference in distribution between the resin and glass microspheres in vertical VFM testing (19.81% vs 24.26%; $P = .182$; n = 18; $P > .05$ by material type per channel).

Correlation of Particle to Fluid Distribution

A moderate correlation between the distribution of microspheres as measured by weight and distribution of injection fluid containing dye was obtained ($r^2 = 0.5712$; n = 144 combined glass and resin injections), but the correlation of microsphere distribution with total fluid volume (BMF plus injection mixture) was poor ($r^2 = 0.0104$; n = 144 combined glass and resin injections; Fig 6).

Effect of Injection Solution Viscosity on Distribution (Glass Only)

The effect of increasing the viscosity of the injection solution by adding contrast agent from 0% to 60% vol/vol showed generally reduced alignment of glass microspheres to total fluid volume for concentrations greater than 30% vol/vol. As shown in Figure 7, the relative alignment is closest to the optimum (ie, 100% alignment of spheres and total fluid volume) at or below approximately 30% contrast medium in saline solution for a fixed injection flow rate of 20 mL/min.

Effect of Injection Solution Flow Rate on Distribution (Dye Only)

Dye-containing injection solution was introduced via the microcatheter at constant flow rates of 5–30 mL/min into the pulsing BMF flow (viscosity, 4 cP) with three injection solution compositions (0%, 30%, and 60% vol/vol contrast agent in saline solution). Dye distribution was used as a surrogate for microsphere distribution, having shown a representative correlation in previous testing. Results indicated that, as the flow rate of the injection solution increased, there was better alignment of injectate distribution relative to the total fluid distribution, approaching unity (Fig 8). For injection of saline solution (viscosity, ~1 cP), the distribution appeared optimal at greater than 10 mL/min.

DISCUSSION

The present study aimed to mimic aspects of hepatic flow during 90Y microsphere therapy, assessing the effects of gravity on microsphere density and bulk flow, injection solution viscosity, and injection flow rate on
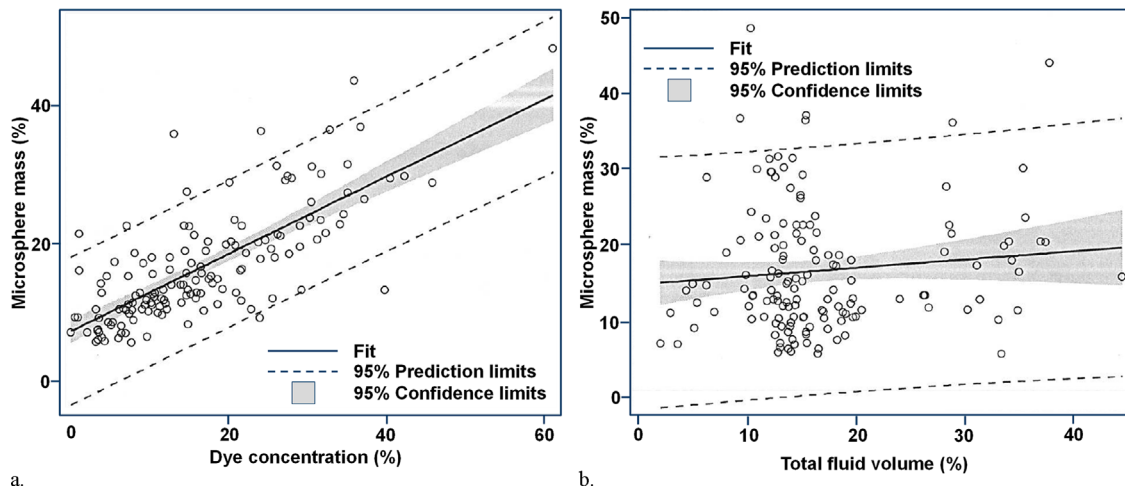
Figure 6. Fit plot for microsphere mass versus dye concentration **(a)** and total fluid volume **(b)** (n = 144 combined injection results with confidence interval shown). Moderate correlation was demonstrated in comparing injection dye and mass ($r^2 = 0.5712$), but a poor correlation was seen between microsphere mass and total fluid volume ($r^2 = 0.0104$), indicating that dye concentration (injectate phase) is an enhanced indicator of microsphere distribution.
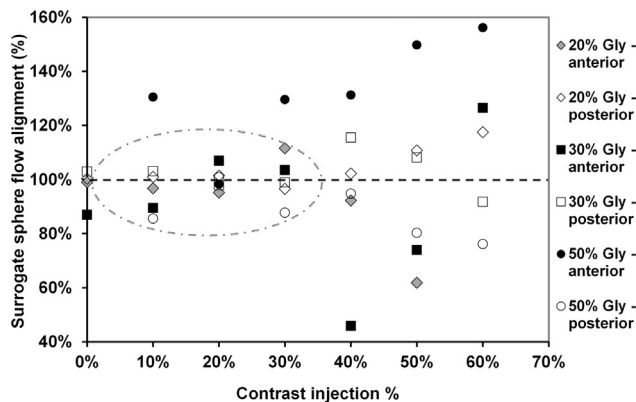

Figure 7. Concentration of glass microspheres (percent per channel divided by total flow percentage) in anterior and posterior channels versus contrast agent dilution. Injection was performed at 20 mL/min into 120 mL/min BMF flow. Hashed ellipse identifies favorable microsphere concentration indicative of enhanced microsphere load delivered in the flow direction.

distribution of resin and glass microspheres. Increased understanding and control of injection parameters could potentially yield more predictable microsphere distribution and improved patient outcomes.

Observations with the VFM in vertical and horizontal orientations showed that the resin and glass microspheres had substantially equivalent distribution (**Figs 4, 5**). Gravitational sedimentation was not observed with either surrogate material. There was a gravitational effect on the total volume flow from each channel with the VFM in the vertical orientation, with increased BMF flowing to the posterior channels. This finding correlates with studies performed in vivo on posture-related blood distribution (33,34).

Reducing the BMF flow rate to 60 mL/min, intended to test gravitational effects, consistently showed equivalent microsphere distributions for glass and resin. This

finding aligns with previous work (8), and serves to highlight the minimal influence of microsphere density even in reduced flow conditions.

Sedimentation theory explains the lack of gravitational effect under the tested conditions. The critical sedimentation velocity can be calculated for a microsphere of a known density and size relative to the bulk fluid properties (21). The critical sedimentation velocities for the glass and resin microspheres in BMF are 0.16 mm/s and 0.045 mm/s, respectively, far lower than the BMF flow rate of 79–159 mm/s (60–120 mL/min) under test conditions. Therefore, the effect of microsphere density on distribution is trivial in this model, in which the flow behavior is dominated by the BMF viscosity, flow rate, and channel geometry. The density of the microsphere may become more important when the blood flow becomes significantly reduced, as when approaching stasis. This would be more relevant for resin spheres because of the minimally embolic nature of glass microsphere treatment (11).

Many studies have evaluated the factors affecting microsphere distribution by using computational fluid dynamics simulations (6,10,19,20,35). Basciano et al (18) showed that microparticles injected into a computational fluid dynamics–simulated vasculature would tend to follow a "flow stream" within the blood vessels. Treatment of diffuse, hypervascular hepatocellular carcinoma lesions requires sufficient mixing of microspheres, as microspheres following a single-directional flow stream could result in nonuniform radiation dose. Recently, Jernigan et al (36) studied the propagation of resin and glass microspheres in a two-dimensional in vitro "river delta" model that suggested that resin microspheres penetrated further while also demonstrating no influence of gravity, leaving some questions as to the defining forces affecting microsphere distribution (eg, viscous drag, density, and injection rate). In contrast, Basciano
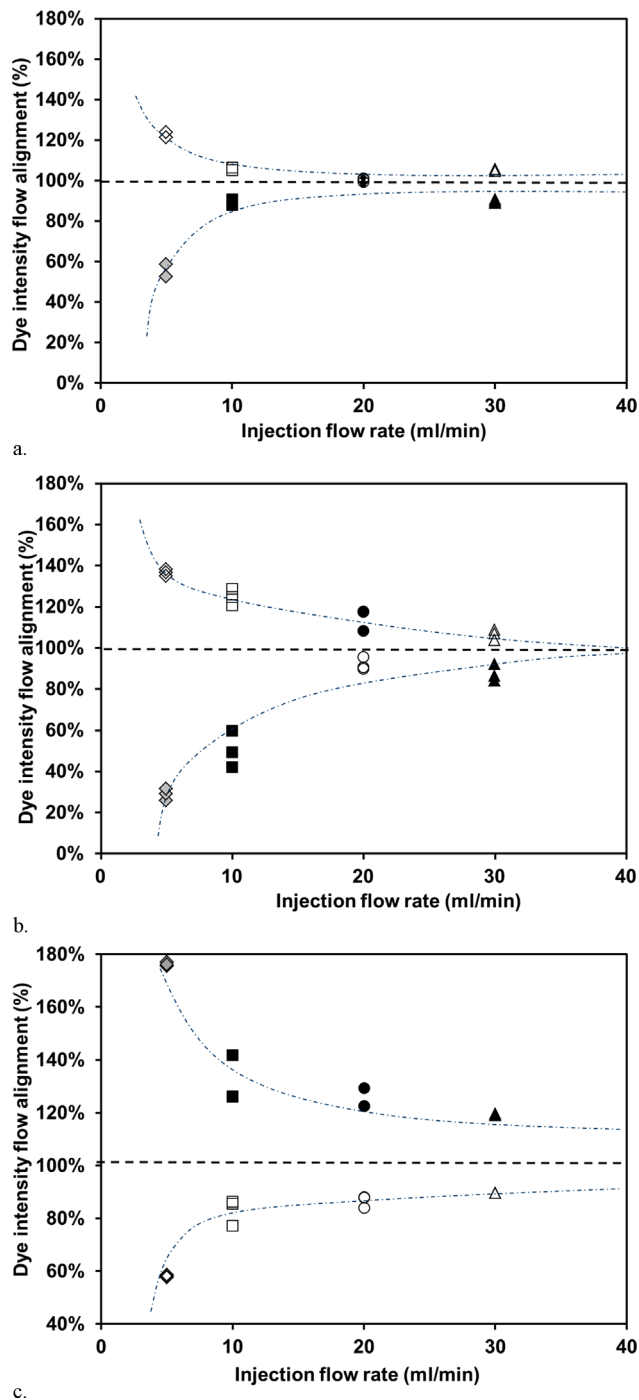
Figure 8. Concentration percentage of dye in anterior (solid) and posterior (outline) channels divided by the total flow volume percentage per channel versus injection flow rate (n = 2 replicates at each condition), with a target of 100% optimal flow alignment (dashed line). Separate graphs indicate contrast agent concentrations in injection solution: 0% vol/vol **(a)**, 30% vol/vol **(b)**, and 60% vol/vol **(c)**.

et al (6) found that a greater than 10-fold difference between fluid and microsphere density is required to influence microsphere sedimentation.

Microsphere distribution correlated poorly with total fluid volume; rather, the data suggest that distribution is better predicted by the dyed injection solution. This is contrary to the conclusion of some studies that showed injected microspheres fully correlating with the total blood flow, with microsphere distribution assessed by ^{90}Y positron emission tomography/CT imaging (8,13,14). Other studies would seem to agree with the present findings, such as recent computer simulations (6,10,19) that showed injection and bulk flow rates to be critical factors affecting distribution of microspheres. It seems reasonable that the degree of mixing of the injection solution and BMF will ultimately determine the homogeneity of the microsphere distribution.

The present study examined whether modifying the viscosity of the injection solution to more closely match the viscosity of the BMF would result in enhanced mixing of the two fluids (22), resulting in increased alignment with the bulk flow. Tests showed a less promising effect whereby contrast medium concentrations greater than 30% vol/vol produced diminishing levels of microsphere mixing with the BMF. This observation correlates with those of another in vivo blood flow study (30) in which > 30% vol/vol contrast medium dilution resulted in increased shear-associated erythrocyte aggregation in microvascular blood flow. Increasing the viscosity of the injection solution, particularly with a higher-viscosity BMF, may cause the mixing process to be inhibited and yield incomplete mixing. Considering two-phase viscous flow, a solution of increasing viscosity will move more slowly and limit the diffusion capabilities of particles contained within that fluid (22). Contrast medium concentrations as high as ∼30% vol/vol may yield satisfactory mixing, and may have some utility in visualizing the flow with angiographic imaging techniques. Recent studies (37) used up to 50% vol/vol dilution of Isovue (Bracco, Milan, Italy) during resin delivery, although the ionic strength of the contrast agent was unreported (potential range of 3.3–20.9 cP viscosity). The viscosity of the 50% Isovue is similar to the viscosity of the 0%–30% vol/vol Omnipaque range presented for the present study, with encouragingly similar results. However, it must be noted that, in the present study, the pure saline solution injection yielded the greatest microsphere alignment with bulk flow under the tested range of injection conditions.

Injection flow rate is understood to be important to solution mixing (6,10,19). In the present study, the use of an injection flow rate of greater than 10 mL/min was shown to yield substantial alignment with the bulk flow in a range of BMF conditions when saline solution was the injection solution. Increasingly viscous contrast agent mixtures required a greater injection flow rate to achieve comparable levels of distribution. High-speed video was used to observe the mechanics of mixing at the VFM inlet and first bifurcation and observe flow streams (**Fig 3**). At lower injection rates (5–10 mL/min) and a BMF flow rate of 120 mL/min, there was a clearly visible laminar stream of injection solution providing evidence

of inadequate mixing (Fig E1 [available online at www.jvir.org]). As the viscosity of the injection solution was increased, higher injection flow rates were required to achieve satisfactory mixing. An explanation for the importance of flow is offered by jet mixing theory, whereby the input flow rate (at the catheter tip) must overcome the bulk flow inertia and viscous drag forces to enable effective radial mixing (23,24).

The present study has several limitations. The first is that the VFM is not fully representative of the complexities of a liver vascular network. The VFM is a scaled two-dimensional representation of a first-order hepatic network (16) that is suitable for comparative results between the outlet channels. The BMF viscosities investigated included three points in a dynamic range between 3.32 and 9.20 cP using a Newtonian fluid BMF. This is therefore a limited simulator of colloidal in vivo blood flow. The injection technique and administration system were taken from the TheraSphere package insert. The pulsed injection technique and administration system for SIR-Spheres was not tested, and this is observed as a limitation. Surrogate materials were selected to represent the size and density of commercially available radioembolic agents; however, nonradiolabeled original products were not available for this study. It is acknowledged that resin microspheres are administered with water or dextrose 5% in water (SIR - Spheres microspheres [Yttrium-90 Microspheres] [package insert]; 38,39) and not saline solution, and that microsphere injection volumes were standardized in this study to avoid volume bias despite being observed to vary in clinical practice, with resin treatments typically involving 10–40 million microspheres versus 1–8 million microspheres for glass. The catheter tip was not mechanically fixed in position near its tip, even though efforts were made to standardize the tip position and angle during testing. Although it is likely that a concentration of as much as 30% vol/vol contrast medium would be visible with existing angiographic imaging techniques, concurrent contrast medium and microsphere injection is not currently indicated for either microsphere product (TheraSphere Yttrium-90 Glass Microspheres [package insert], SIR - Spheres microspheres [Yttrium-90 Microspheres] [package insert]).

The present study investigated several parameters affecting microsphere distributions in an in vitro flow model mimicking radioembolic therapy to the liver. No significant difference in flow distribution was observed in terms of surrogate material density. It was observed that injection solution distribution was a better predictor of microsphere deposition than total fluid volume. Injection rates greater than 10 mL/min were found to enhance mixing, aligning more closely to bulk fluid flow. Injections solutions could also be modified with as much as 30% vol/vol contrast agent for potential visualization of the flow with angiographic techniques; however, increasing the concentration of contrast medium to more than 30% vol/vol resulted in significant loss of microsphere flow alignment.

REFERENCES

1. Hilgard P, et al. Radioembolization with yttrium-90 glass microspheres in hepatocellular carcinoma: European experience on safety and long-term survival. Hepatology 2010; 52:1741–1749.
2. Morgan B, et al. Intra-arterial brachytherapy of hepatic malignancies: watch the flow. Nat Rev Clin Oncol 2011; 8:115–120.
3. Gates VL, et al. Radioembolization with Yttrium-90 microspheres: review of an emerging treatment for liver tumors 2007.
4. Ariel IM. Treatment of inoperable primary pancreatic and liver cancer by the intra-arterial administration of radioactive isotopes (Y90 radiating microspheres). Ann Surg 1965; 162:267.
5. Salem R, Mazzaferro V, Sangro B. Yttrium 90 radioembolization for the treatment of hepatocellular carcinoma: biological lessons, current challenges, and clinical perspectives. Hepatology 2013; 58:2188–2197.
6. Basciano CA, Kleinstreuer C, Kennedy AS. Computational fluid dynamics modeling of 90Y microspheres in human hepatic tumors. J Nucl Med Radiat Ther 2011; 2:2.
7. Erbe EM, Day DE. Chemical durability of Y2O3-Al2O3-SiO2 glasses for the in vivo delivery of beta radiation. J Biomed Mater Res 1993; 27:1301–1308.
8. Ibrahim SM, et al. Radiographic response to yttrium-90 radioembolization in anterior versus posterior liver segments. Cardiovasc Intervent Radiol 2008; 31:1124–1132.
9. Kennedy AS, et al. Computer modeling of yttrium-90–microsphere transport in the hepatic arterial tree to improve clinical outcomes. Int J Radiat Oncol Biol Phys 2010; 76:631–637.
10. Walrand S, et al. The low hepatic toxicity per gray of 90Y glass microspheres is linked to their transport in the arterial tree favoring a nonuniform trapping as observed in posttherapy PET imaging. J Nucl Med 2014; 55:135–140.
11. Lam MG, et al. Root cause analysis of gastroduodenal ulceration after yttrium-90 radioembolization. Cardiovasc Intervent Radiol 2013; 36:1536–1547.
12. Kokabi N, et al. A simple method for estimating dose delivered to hepatocellular carcinoma after yttrium-90 glass-based radioembolization therapy: Preliminary results of a proof of concept study. J Vasc Interv Radiol 2014; 25:277–287.
13. Beck KC. Regional trapping of microspheres in the lung compares well with regional blood flow. J Appl Physiol 1987; 63:883–889.
14. Domenech RJ, et al. Total and regional coronary blood flow measured by radioactive microspheres in conscious and anesthetized dogs. Circ Res 1969; 25:581–596.
15. Kerlan RK Jr. Chapter 19–Diagnostic angiography in hepatobiliary and pancreatic disease: Indications A2–Jarnagin, William R. In: Blumgart LH, editor. Blumgart's Surgery of the Liver, Pancreas and Biliary Tract (Fifth Edition). Philadelphia: W.B. Saunders; 2004; 345–356.e1.
16. Van Der Plaats A, et al. Numerical simulation of the hepatic circulation. Int J Artif Organs 2004; 27:222–230.
17. Irie T, Kuramochi M, Takahashi N. Diameter of main tumor feeding artery of a hepatocellular carcinoma: Measurement at the entry site into the nodule. Hepatol Res 2015.
18. Basciano C, et al. Computer modeling of controlled microsphere release and targeting in a representative hepatic artery system. Ann Biomed Eng 2010; 38:1862–1879.
19. Richards AL, et al. Experimental microsphere targeting in a representative hepatic artery system. Biomedical Engineering, IEEE Transactions on 2012; 59:198–204.
20. Kleinstreuer C, et al. A new catheter for tumor targeting with radioactive microspheres in representative hepatic artery systems. Part I: Impact of catheter presence on local blood flow and microsphere delivery. J Biomech Eng 2012; 134:051004.
21. Steinour HH. Rate of sedimentation. Nonflocculated suspensions of uniform spheres. Ind Eng Chem 1944; 36:618–624.
22. Yager P. Transverse diffusion in microfluidic systems. Lab-ona-chip: Chemistry in Miniaturized Synthesis and Analysis Systems 2003.
23. Elrod, Heat. Piping Air Cond 1954; 26:149–155.
24. Mohan ND, Prakash K, Panchapakesan N. Mixing augmentation by multiple lobed jets. Am J Fluid Dyn 2015; 5:55–64.

25. Fung Y-C. Biomechanics: Circulation. Springer Science & Business Media; 1997.
26. Banerjee MK, Ganguly R, Datta A. Effect of pulsatile flow waveform and Womersley number on the flow in stenosed arterial geometry. ISRN Biomathematics 2012.
27. Schetz JA, Fuhs AE. Fundamentals of fluid mechanics. John Wiley & Sons; 1999.
28. Yousif M, Holdsworth D, Poepping T. A blood-mimicking fluid for particle image velocimetry with silicone vascular models. Experiments in Fluids 2011; 50:769–774.
29. Kanaris A, Anastasiou A, Paras S. Modeling the effect of blood viscosity on hemodynamic factors in a small bifurcated artery. Chem Eng Sci 2012; 71:202–211.
30. Laurent A, et al. Effects of contrast media on blood rheology: comparison in humans, pigs, and sheep. Cardiovasc Intervent Radiol 1999; 22:62–66.
31. Salem R, et al. Technical aspects of radioembolization with 90 Y microspheres. Tech Vasc Interv Radiol 2007; 10:12–29.
32. Schenk WG Jr, et al. Direct measurement of hepatic blood flow in surgical patients: with related observations on hepatic flow dynamics in experimental animals. Ann Surg 1962; 156:463.
33. Taniguchi H, et al. Difference in regional hepatic blood flow in liver segments—Non-invasive measurement of regional hepatic arterial and portal blood flow in human by positron emission tomography with H2 15O—. Ann Nucl Med 1993; 7:141–145.
34. Olufsen MS, et al. Blood pressure and blood flow variation during postural change from sitting to standing: model development and validation. J Appl Physiol 2005; 99:1523–1537.
35. Kennedy A, Dezarn W, McNeillie P. 90Y Microspheres: Concepts and principles. Springer Berlin Heidelberg; 1–10.
36. Jernigan SR, et al. Selective internal radiation therapy: quantifying distal penetration and distribution of resin and glass microspheres in a surrogate arterial model. J Vasc Interv Radiol 2015.
37. Chao C, et al. Effect of substituting 50% isovue for sterile water as the delivery medium for SIR-SPHERES: improved dose delivery and decreased incidence of stasis. J Vasc Interv Radiol 2014; 25: S89.
38. Ahmadzadehfar H, et al. Evaluation of the delivered activity of yttrium-90 resin microspheres with sterile water and 5% dextrose (D5W) as application agents. Eur J Nucl Med Mol Imaging 2015; 42: S744–S745.
39. Paprottka KJ, et al. Reduced peri-procedural analgesia following replacement of water for injection (WFI) with glucose 5%(G5) solution as the infusion medium for 90 yttrium resin microspheres. J Nucl Med 2016, p. jnumed. 115.170779.

APPENDIX A. SUPPLEMENTARY METHODS

1: Pressure Profile of Blood Mimicking Fluid Pump And Calculated Pulsatility (Womersley Number)

A human vasculature is subject to pulsing blood flow, with expected implications in mixing of the injection solution (containing microspheres) with the blood. The pulsatile motion of the blood-mimicking fluid (BMF) in the present study was intended to mimic mixing conditions in a liver right hepatic artery. A pressure plot was generated for the 4-mm inlet channel of the vascular flow model (VFM) using a research-grade blood pressure transducer (220v; Harvard Apparatus UK, Cambridge, United Kingdom), data-acquisition signal board (NI USB-6009; National Instruments, Austin, Texas), and custom MatLab acquisition code (MathWorks, Natick, Massachusetts), as shown in Figure E1. The plot shown is for BMF composed of a 44%:56% vol/vol glycerol: water mixture modified with 15% sodium iodide with a dynamic viscosity of 4.51 cP, with BMF nominally circulating at 120 mL/min.

The analysis of the influence of pulsatile flow on mixing uses a dimensionless value known as the Womersley number (denoted α), a relative measure of the mixing potential of injectate and blood (26). The Womersley number is defined by the following equation:

$$\alpha = L\left(\frac{\omega \rho}{\eta}\right)1/2$$

Equation 1: Equation for Womersley number representative of flow pulsatility.

where L is the appropriate channel length scale, ω is the angular frequency of a pulse waveform taken from a pressure plot, ρ is fluid density, and η is the kinematic viscosity term.

This value can be applied to the pulsatile waveform to analyze the influence of pulsatile mixing. The 4-mm-diameter inlet channel of the VFM used here has an α of 2.2–3.9 with ω of 10.47 at a BMF viscosity range of 3.03–9.89 cP over a time period of 0.6 seconds. The reported Womersley number for human vascular systems is between 0.04 in arterioles and 4.4 in the larger carotid artery (25,26), and therefore the pulsatility of the tested system is within the biologic range appropriate to hepatic lobar vasculature.

2: Catheter Tip Alignment

Previous work (17–19) has shown the importance of catheter tip orientation relative to the "blood vessel" on microsphere distribution. Effort was made to ensure that the straight (end-hole) catheter tip was centered inside the VFM inlet channel and aligned with the axis of the flow channel. In addition, the entrance length of the inlet channel, measured from the tip of the catheter to the first bifurcation, was controlled to ensure that there would be adequate opportunity for the injectate and microspheres to completely mix with the BMF before reaching the first bifurcation. Entrance length required for fully developed flow in laminar conditions is defined as follows (27):

$$L_e/D = 0.6 + 0.056Re$$

Equation 2: Entrance length equation for fully developed flow profile.

where L_e is entrance length, D is channel diameter, and Re is Reynolds number. For the VFM and BMF range (Reynolds number, 37–226) under test, maximum entrance length of 53 mm at maximum flow rate 120 mL/min at Reynolds number 226. The catheter tip
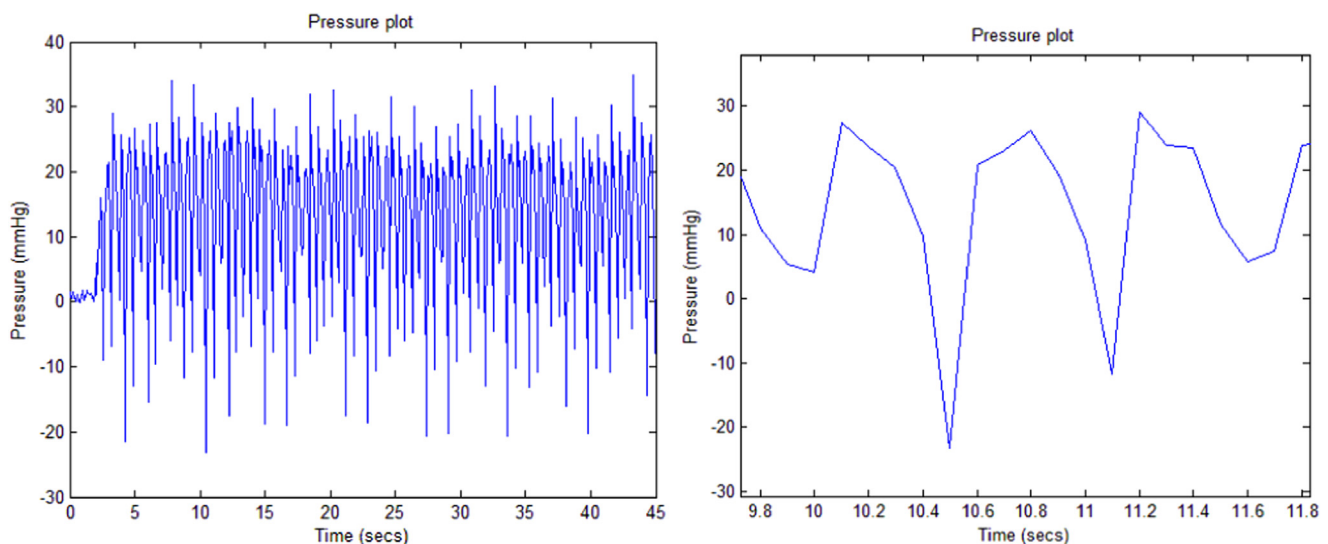

Figure E1. Pressure plot for inlet pulsatile pressure for calculation of angular pulse frequency (ω; left) and waveform profile for a single pump cycle (right).

position was fixed at a point greater than 53 mm from the first bifurcation.

3: Critical Sedimentation Velocity

An explanation for the equivalent flow behavior of the two microsphere materials (particles of similar size but quite different densities) can be found in sedimentation theory. The critical sedimentation velocity (*vs* in **Eq. 3**) as a function of the microsphere and BMF density is given by the following (25):

$$vs = \frac{2g(\rho_p - \rho)r_p^2}{9_\mu}$$

Equation 3: Critical setting velocity equation for spheres in fluid flow.

where g is the gravitational constant (9.81 m/s^2), ρ_p is the particle density (glass, 3.29 g/cm^3 [8]; resin, 1.6 g/cm^3 [9,10]), ρ is fluid density (1.24 g/cm^3, measured for BMF composed of a 44%:56% vol/vol glycerol:water mixture modified with 15% sodium iodide), r_p is the mean particle radius (glass, 25 µm [TheraSphere, Biocompatibles UK, Farnham, United Kingdom]; resin average, 32 µm [SIR-Spheres; Sirtex, North Sydney, Australia]), and µ is the fluid dynamic viscosity (0.0045 kg/m·s) as measured by using an automated microviscometer (AMVn2-PA, 1.8-mm capillary; Anton Paar, Ostfildern-Scharnhausen, Germany]).

For glass spheres:

$$\text{Glass } vs = \frac{2(9.81)(3300-1240)25^2}{9(0.0045)} = 0.16 \text{ mm/s}$$

For resin spheres:

$$\text{Resin } vs = \frac{2(9.81)(1600-1240)32^2}{9(0.0045)} = 0.045 \text{ mm/s}$$

This calculation predicts a higher sedimentation rate at lower fluid velocities for the denser glass microspheres purely as a function of material properties. The critical sedimentation velocities for the glass and resin microspheres in BMF are 0.16 mm/s and 0.045 mm/s, respectively, far lower than the BMF velocity of 79–159 mm/s (60–120 mL/min) under test. This would suggest that settling will not be a dominant force to determine distribution within the VFM.

4: Two-Phase Viscous Flow Theory, Mixing, And Relative Injection Flow Rate

One of the hypotheses of the present study was that, by modifying the viscosity of the injection solution to more closely match the viscosity of the BMF, that advective (ie, turbulent) mixing of the fluids would be enhanced and could potentially be optimized. Another hypothesis was that modifying the flow rate of the injection solution could
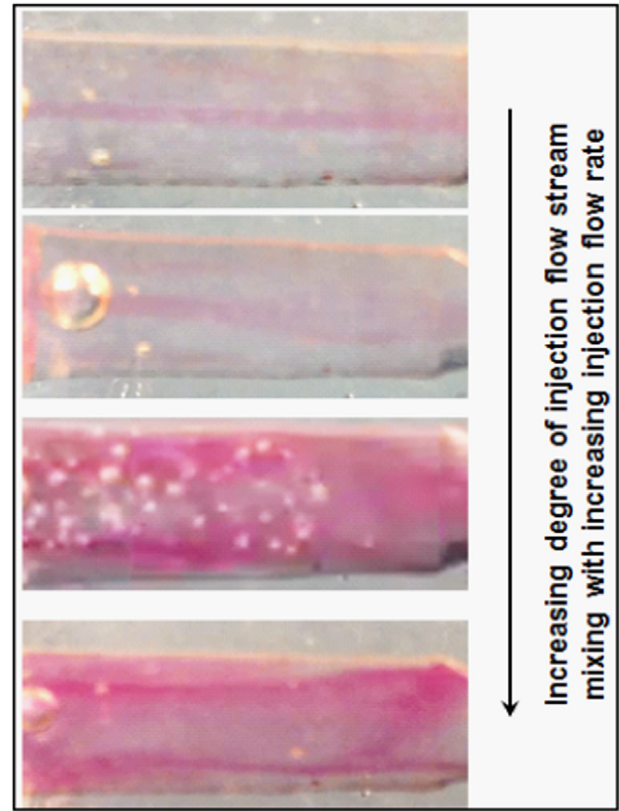

Figure E2. Flow streams in the VFM inlet (20% glycerol BMF; 120 mL/min) with injection flow rates of 5 mL/min (top), 10 mL/min, 20 mL/min, and 30 mL/min (bottom) of injection solution with dye (60% contrast medium). Images acquired at "systole" phase of pump cycle during injection.

be optimized to enhance mixing. In testing, it was found that increasing the injection solution viscosity yielded reduced flow miscibility, in that there was greater viscous resistance to advective flow mixing. In contrast, increasing the injection flow rate from the catheter appears to provide increased advective mixing and particle dispersion throughout the flow channel. These effects are described by jet mixing theory, whereby the input flow velocity must override the BMF bulk flow fluidic conditions (inertia/viscosity) to enable effective mixing within the inlet channel (32,33). Adding contrast medium to the injection solution serves to increase the density and viscosity of the injection solution, thereby slowing the relative velocity and restricting the radial mixing in the entrance channel (30).

High-speed video of the inlet channel immediately downstream of the catheter tip was used to visualize the effects of injection velocity (**Fig E2**). With insufficient injection velocity, the injectate (colored with red Safranin O dye) will follow a single flow stream, whereas increased velocity yields turbulent mixing of the injectate with the BMF and increases mixing of injection solution.